Supplementary Materials for

Epithelial integrity monitoring via ligand-receptor segregation ensures malignant cell elimination

Geert de Vreede[1], Stephan U. Gerlach[1] and David Bilder[1*]

Correspondence to: bilder@berkeley.edu

This PDF file includes:

Materials and Methods

Figs. S1 to S9

Tables S1 to S3

MATERIALS AND METHODS

Drosophila genetics

Experimental crosses were raised at 25°C in uncrowded conditions. *yw* flies were used for WT controls. ptc^{ts} crosses were shifted to 29°C ~72 hours after egg laying (AEL). ptc^{ts}*>dlgKD* does not trigger wing pouch apoptosis at 25°C. *FLPout dlg KD* clones in **Fig. 1 B-D** and **Fig. S1A-C** were induced via a single 15-minute heat shock at 48 ± 12 hours AEL, returned to 18°C, then shifted to 29°C 24 hours before dissection. For **Fig. S1K** and **Fig. S5A, B**, larvae were dissected 12 hours after the 29°C shift. *scrib* mitotic clones in **Fig. 2E-K** and **Fig. S1G** were induced via two 45-minute heat-shocks at 60 ± 12 hours AEL and dissected as late L3 larvae. *FLPout Myc O/E* clones in **Fig. S1H** were induced via a single 20-minute heat shock at 48 ± 12 hours AEL and dissected as late L3 larvae. *scrib* tumor-bearing larvae were staged by a 24-hour egg collection and dissected 8 days AEL. egr^{1} and egr^{3} alleles did not contain *NimC1* mutations (*23*, *24*). Other transgenic lines and alleles used were: *UAS-Egr-Venus* (*14*), *egr-LacZ* (*16*), *AP-1-GFP/RFP* (*25*), $UAS\text{-}aPKC^{\Delta N}$ (*26*), *5xQEdsRed* (*27*), *Tub> Myc* y^{+} *>Gal4* (*28*), *UAS-Grnd-V5* (*8*), $scrib^{1}$ and $scrib^{2}$ (*29*). *UAS-Egr RNAi (45252), UAS-Dlg RNAi (41136) UAS-Grnd-RNAi (104538), UAS-Tak1 RNAi (101357)* were obtained from the Vienna Drosophila RNAi Center. *hsFLP; Act>CD2>Gal4 UAS-RFP/S-T, UAS-GFP*, *UAS-hisRFP*, *Tub-Gal4*, *Tub-Gal80TS*, *Act-Gal4, ptc-Gal4, R4-Gal4, Ppl-Gal4, CG-Gal4, Nub-Gal4, Hh-Gal4, En-Gal4, Hml*Δ*-Gal4, MS1096-Gal4,* $HSflp^{122}$*,* $UAS\text{-}Hep^{WT}$*,* $UAS\text{-}Ras^{V12}$*,* $UAS\text{-}bsk^{DN}$*, w*; *FRT82,* Egr^{GFSTF}*, UAS-GrabFP-Vkg-mCherry,* $UAS\text{-}GrabFP\text{-}Apical^{Ext}\text{-}mCherry$*, UAS-Dlg RNAi (39035), UAS-Cor RNAi (35003), UAS-Vps16 RNAi (38271), UAS-Egr RNAi (55276), UAS-Shi RNAi (36921), UAS-Wengen RNAi (50594)* were obtained from the Bloomington Stock Center. See **Table S1** for key resources, including fly stocks. See **Table S2** for genotypes of experimental crosses.

Co-culture experiments

Larval fat bodies expressing Venus-tagged Egr (*R4-Gal4 UAS-Egr-Venus*) were dissected and cultured in a small volume of Schneider's medium (Gibco) supplemented with 10% FBS (Gibco) and 1% Pen/Strep

(Caisson Labs) for 2.5 hours at 29°C. At least 12 larval imaginal discs of indicated genotypes were dissected and added to this mixture and co-cultured for 5 hours at 29°C. For **Fig. 1B-D**, and **Fig. S1A-C, G-H, K**, clones were induced as indicated above and subsequently co-cultured. Co-culture experiments were performed at 29°C to increase fat body EgrV expression.

Immunofluorescence and microscopy

Larval imaginal discs and fat bodies were dissected, fixed in 4% PFA for 20 minutes, blocked and stained using standard procedures. The following primary antibodies and dilutions were used: mouse anti-Grnd 1:500 (7D9)(*8*), mouse anti-Dlg 1:100 (DSHB, 4F3), mouse anti-V5 1:500 (Invitrogen), mouse anti-Coracle 1:500 (DSHB C566.9), mouse anti-Notch-ECD 1:25 (DSHB C458.2H), mouse anti-Hemese 1:100 (From I. Ando) (*30*), rabbit anti-DCP-1 1:300 (Cell signaling), rabbit anti-PH3 1:300 (Cell signaling), rabbit anti-GFP 1:500 (Torrey Pines), rabbit anti-β-gal 1:1000 (Abcam). Secondary fluorophore-conjugated antibodies (Molecular Probes) were used at 1:250. TRITC-phalloidin was used to visualize F-actin (1:500, Sigma) and DAPI (1:1000) was used to visualize DNA. To ensure staining in the core as well as periphery of *scrib* tumors, permeabilization and blocking buffers were used with 1% Triton X-100 and were incubated rocking at 4°C for 96 hours in primary and 48 hours in secondary antibody. See **Table S1** for key resources, including antibodies. Confocal images were obtained on either a Zeiss LSM 700 confocal microscope or a Zeiss LSM 780 confocal microscope. Images were processed in Fiji (*31*) and Adobe Photoshop CC. All data were collected as images with 16-bit per channel.

Wounding and bleeding

Wounding experiments used L3 larvae containing either *nub-Gal4 UAS-RFP, hh-Gal4 UAS-RFP* or *5xQEdsRed* to mark the wing imaginal discs. Animals were immobilized in ice cold PBS, and the wing epithelium was wounded by applying pressure on RFP marked tissue using a blunted tungsten needle without disrupting the larval cuticle. To obtain hemocyte samples, at least 10 larvae were washed in PBS

and ethanol, and larval cuticles were punctured with a sharp, sterile tungsten needle. Larvae were bled on a slide coated with poly-D-lysine and after removal of carcasses the hemocytes were fixed on the slide for 5 min with 4% PFA.

Endocytosis and Dextran assays

For Notch endocytosis assays, wing imaginal discs were dissected in ice cold Schneider's medium (Gibco) supplemented with 10% FBS (Gibco) and 1% Pen/Strep (Caisson Labs). Discs were pulsed for two hours at 4°C with mouse anti-Notch-ECD (1:50) in Schneider's medium. Samples were subsequently washed, chased in Schneider's at room temperature and fixed with 4% PFA at the indicated time points. For Dextran endocytosis assays, discs were pulsed with 3kD FITC Dextran (1mg/ml, Invitrogen) for 10 minutes at 25°C in Schneider's, followed by a 25-minute chase at 25°C. For Dextran permeability assays, wing imaginal discs were cultured in Schneider's medium (Gibco) supplemented with 10% FBS (Gibco) and 1% Pen/Strep (Caisson Labs) with 40kD or 70kD Fluorescein Dextran (1mg/ml, Invitrogen) for 2 hours at 29°C, washed and fixed in 4% PFA.

Quantifications

Fiji (*31*) was used to measure mean fluorescence intensities, areas, volumes, and particle numbers; all measurements were made on 16-bit images. Wing disc measurements analyzed tissue in the pouch. Relative fluorescence quantifications were determined by dividing the mean fluorescence intensities of a manipulated tissue with WT tissue of the same wing disc. Relative DCP-1, EgrV and Grnd fluorescence quantifications with *ptc-Gal4* measured mean fluorescence intensity area and calculated ratios of average intensity of middle third by that of outer thirds. DCP-1 measurements subtracted background signal from fluorescence intensities before calculating ratios. Relative *ptc* stripe size reflects *ptc* tissue area measured via anti-Dlg staining divided by remaining area. Relative AP-1-GFP fluorescence quantifications with *Hh-Gal4* reflect mean fluorescence intensity in posterior compartment divided by anterior compartment.

Relative EgrV and Grnd fluorescence quantifications in clones reflect mean fluorescence intensity of clones divided by mean fluorescence intensity of WT tissue. Relative clone area quantifications in **Fig. 1F** reflect size of RFP-positive clones divided by the entire area. Relative clone area quantifications in **Fig. 2L** reflect size of RFP-negative clones divided by area of sibling RFP-positive clones. EgrV and ANF binding to wounded and unwounded discs reflect mean fluorescence intensities. To assess *egr* expression with *EgrLacZ,* mean fluorescence intensities were measured per hemocyte or fat body cell and the mean value per animal or bleed calculated, representing one data point. EgrV binding to *scrib* tumors reflects mean fluorescence intensities of the entire wing disc. To evaluate *scrib* tumor peripheral versus core AP-1-RFP and DCP-1 signal as well as PH3+ cells, single X-Y sections through the tissue center were used to measure mean fluorescence intensities and count positively marked cells respectively. Periphery was defined as area 20 µm inside the tissue border, while core tissue was defined as the remaining area. See **Table S3** for type of individual units used per quantification. All measurements were taken from multiple samples, no assumptions or corrections were made.

Statistics

Graphpad Prism and Microsoft Excel were used for statistical analysis and graphs. Scatter dot-plots show the mean as columns with error bars indicating the standard deviation. Each experiment was performed at least three times. Two-sided Student's T-test, one-way ANOVA test and the Chi squared test were used to determine statistical significance for two-sample comparisons, multiple sample comparisons and distribution of adult wounding phenotypes respectively. For all two-sample comparisons and multiple sample comparisons, statistical significance was indicated with *$p \leq 0.05$, **$p \leq 0.01$, ***$p \leq 0.001$. Two-sided Student's T-test was used in **Fig. S1F, I, J, L, Fig. S2E, F, Fig. S4F, I, J, Fig. S5E, H, K, Fig. S6F, P, Q, Fig. S7J**, and **Fig. S9B.** One-way ANOVA test was used to determine statistical significance in **Fig. 1E, F, L, Fig. 2D, L, Fig. 4H, I, L, Fig. S2H, Fig. S3E, I, J, Fig. S5F, M, N, Fig. S6G, K,** and **Fig. S9E**. Statistical significance of the wounding response in **Fig. S2K** was determined by Chi-squared test with Bonferroni correction for 7 groups with *$p \leq 0.0024$; **$p \leq 0.00048$; ***$p \leq 0.00005$. See **Table S3** for n and p values

for each statistical test.

SUPPLEMENTAL FIGURES

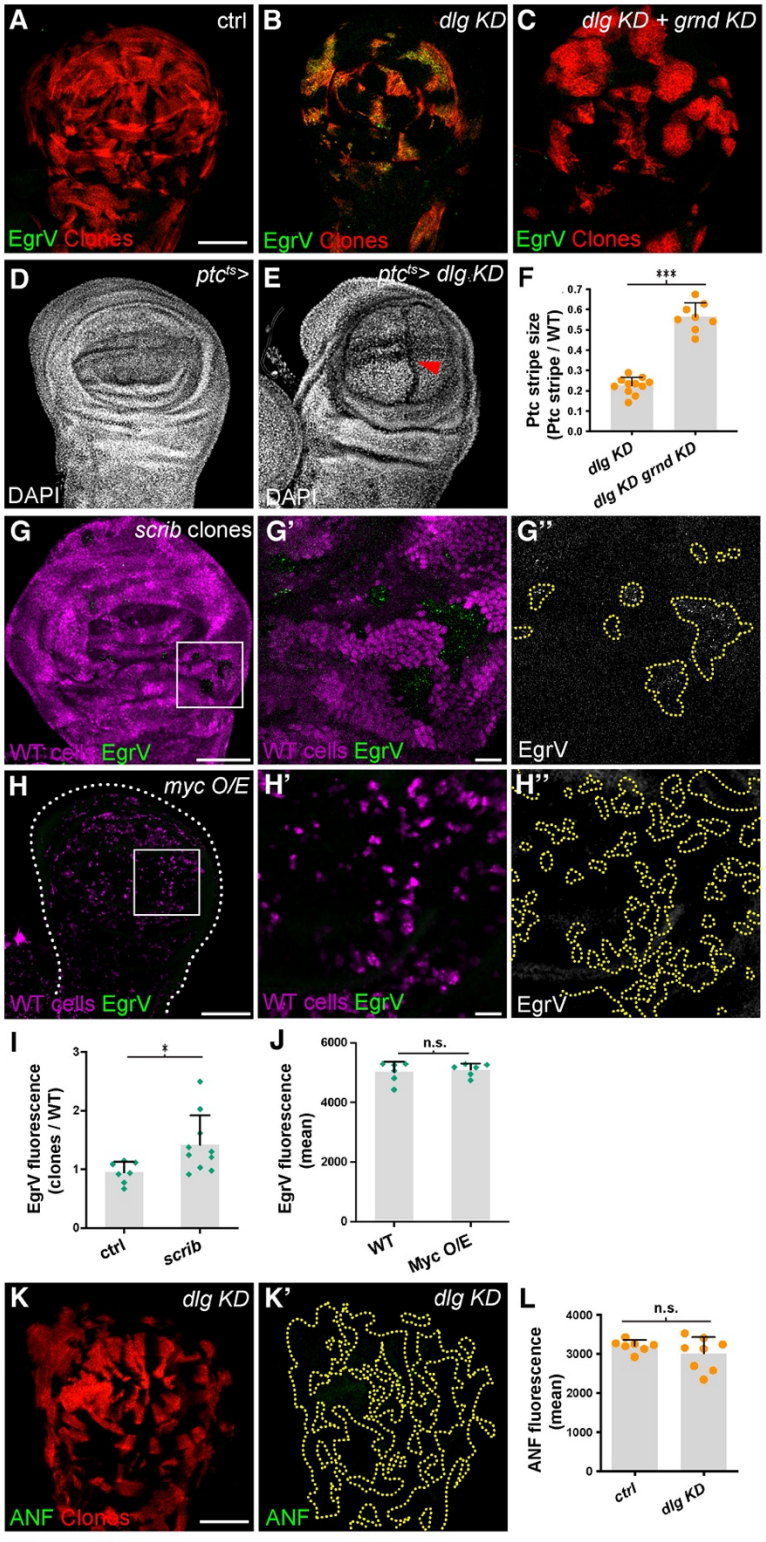

Figure S1

Fig. S1 Egr binds to polarity-deficient cells but not other loser cells

(A-C): Polarity-deficient cells require Grnd to bind EgrV. The border of RFP-positive clones corresponds to dotted lines in **Fig. 1B-D**.

(D-E): Single DAPI channels indicate a fold caused by Dlg depletion. Corresponds to **Fig. 1G, H**.

(F): Depletion of Grnd in polarity-deficient cells causes overgrowth of the Ptc stripe. Corresponds to **Fig. 1J, K**.

(G, I): *scrib* mitotic clones undergoing elimination bind EgrV (**G**), quantitated in **I**.

(H, J): Myc-overexpressing cells that eliminate surrounding WT cells do not induce EgrV binding in losers (**H**), quantitated in **J**.

(K-L): Control secreted protein Atrial Natriuretic Peptide (ANF) fused to GFP does not bind to *dlg*-depleted clones (**K**), quantitated in **L**.

Scale bars: 100 μm in **A, G, H** and **K,** 10 μm in **G'** and **H'**. See Materials and Methods as well as **Table S3** for information on statistical tests.

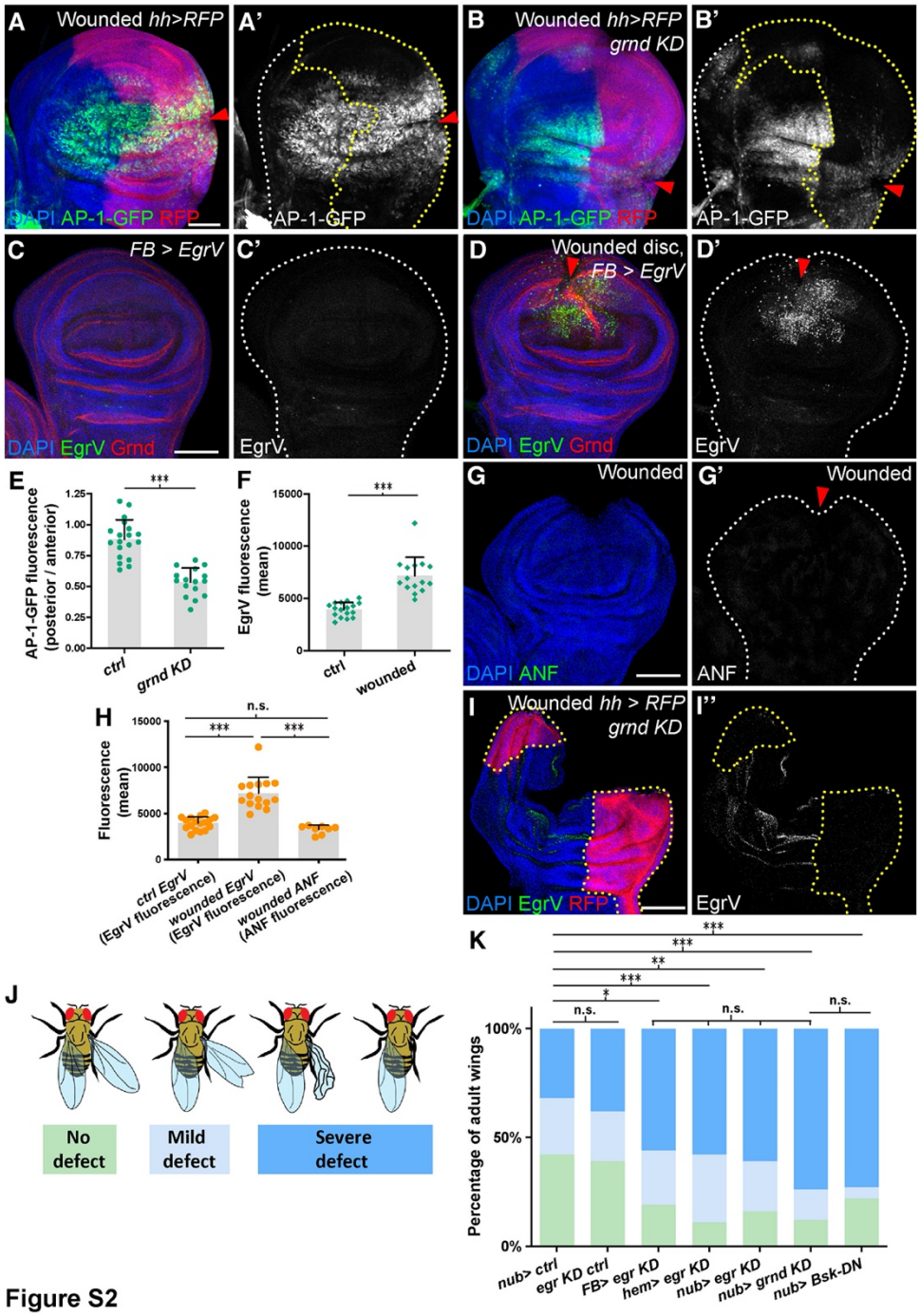
A
Wounded hh>RFP
DAPI AP-1-GFP RFP
A'
AP-1-GFP
B
Wounded hh>RFP
grnd KD
DAPI AP-1-GFP RFP
B'
AP-1-GFP
C
FB > EgrV
DAPI EgrV Grnd
C'
EgrV
D
Wounded disc,
FB > EgrV
DAPI EgrV Grnd
D'
EgrV
E
AP-1-GFP fluorescence
(posterior / anterior)
***
ctrl
grnd KD
F
EgrV fluorescence
(mean)
***
ctrl
wounded
G
Wounded
DAPI ANF
G'
Wounded
ANF
H
Fluorescence
(mean)
n.s.
***
***
ctrl EgrV
(EgrV fluorescence)
wounded EgrV
(EgrV fluorescence)
wounded ANF
(ANF fluorescence)
I
Wounded hh > RFP
grnd KD
DAPI EgrV RFP
I''
EgrV
J
No
defect
Mild
defect
Severe
defect
K
Percentage of adult wings
100%
50%
0%
n.s.
n.s.
n.s.
nub> ctrl
egr KD ctrl
FB> egr KD
hem> egr KD
nub> egr KD
nub> grnd KD
nub> Bsk-DN

Figure S2

Fig. S2 Circulating Egr binds to wounds and is required for efficient wound-healing

(A-F): JNK activation after wounding **(A)** is Grnd-dependent (**B**), quantitated in **E**. The border of *hh-GAL4* expression in the posterior compartment is marked by RFP. EgrV binds to wounded wing discs (**D**, control in **C**), quantitated in **F**.

(G-H): Control secreted protein ANF-GFP does not bind to wounded discs (**G**), quantitated in **H**. Note that first two datasets in **H** are also shown in **F**.

(I): Binding of EgrV to the wound site depends on Grnd (depleted in RFP-expressing cells).

(J-K): Wounding response of wing discs, assayed in adults (**J**). Animals depleted of *egr* in fat body or hemocytes, or *egr, grnd* or *bsk* in the disc, are defective in healing (**K**).

Scale bars: 50 μm in **A** and **C,** 100 μm in **G** and **I.**

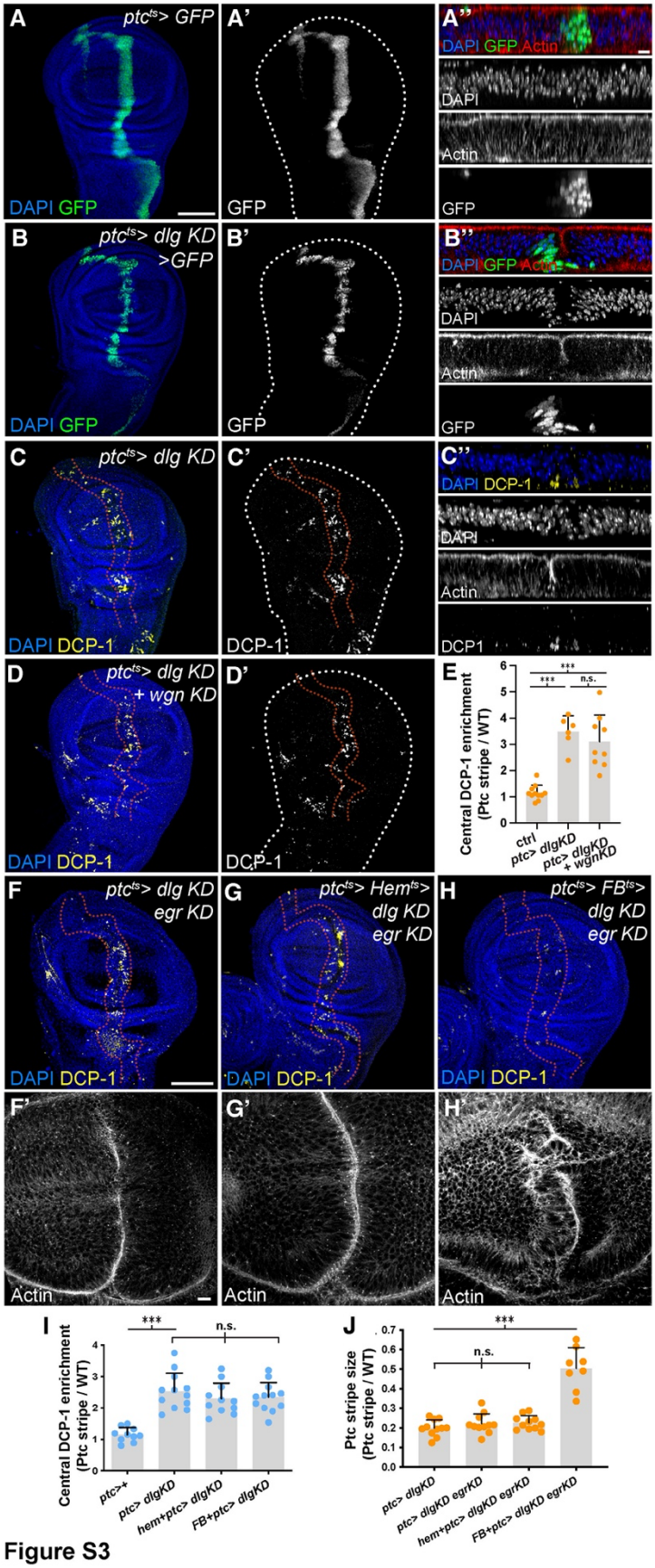
A
ptc^ts> GFP
DAPI GFP
A'
GFP
A''
DAPI GFP Actin
DAPI
Actin
GFP
B
ptc^ts> dlg KD
>GFP
DAPI GFP
B'
GFP
B''
DAPI GFP Actin
DAPI
Actin
GFP
C
ptc^ts> dlg KD
DAPI DCP-1
C'
DCP-1
C''
DAPI DCP-1
DAPI
Actin
DCP1
D
ptc^ts> dlg KD
+ wgn KD
DAPI DCP-1
D'
DCP-1
E
Central DCP-1 enrichment
(Ptc stripe / WT)
***
***
n.s.
ctrl
ptc> dlgKD
ptc> dlgKD
+ wgnKD
F
ptc^ts> dlg KD
egr KD
DAPI DCP-1
G
ptc^ts> Hem^ts>
dlg KD
egr KD
DAPI DCP-1
H
ptc^ts> FB^ts>
dlg KD
egr KD
DAPI DCP-1
F'
Actin
G'
Actin
H'
Actin
I
Central DCP-1 enrichment
(Ptc stripe / WT)
***
n.s.
ptc>+
ptc> dlgKD
hem+ptc> dlgKD
FB+ptc> dlgKD
J
Ptc stripe size
(Ptc stripe / WT)
***
n.s.
ptc> dlgKD
ptc> dlgKD egrKD
hem+ptc> dlgKD egrKD
FB+ptc> dlgKD egrKD

Figure S3

Fig. S3 A consistent system for generating polarity-deficient cell elimination

(A-C): Expression domain of *ptc>GAL4* (**A**) and basal extrusion of dying *dlg*-depleted cells in a stripe along the A-P compartment boundary (**B, C**). Panels on right show X-Z sections through the wing pouch; note the characteristic fold. DAPI indicates nuclei, DCP-1 indicates apoptotic cells.

(D-E): Death of *dlg*-depleted cells does not require the second fly TNFR Wegnen (Wgn) (**D**), quantitated in **E,** ctrl dataset also shown in **Fig. 2D**.

(F-H): While neither depletion of autonomous nor hemocyte-derived Egr suppress apoptosis (**F, G**), depletion of Egr from the fat body suppresses elimination of polarity-deficient cells (**H**) and triggers overgrowth (**H'**), Corresponds to **Fig. 2A-C**.

(I): Depletion of Dlg in hemocytes or fat body does not reduce the apoptotic response at the AP boundary.

(J): Depletion of Egr from the fat body, but not depletion of cell-autonomous nor hemocyte-derived Egr, triggers overgrowth of the Ptc stripe.

Scale bars: 100 μm in **A** and **F**, 10 μm in **A''** and **F'**.

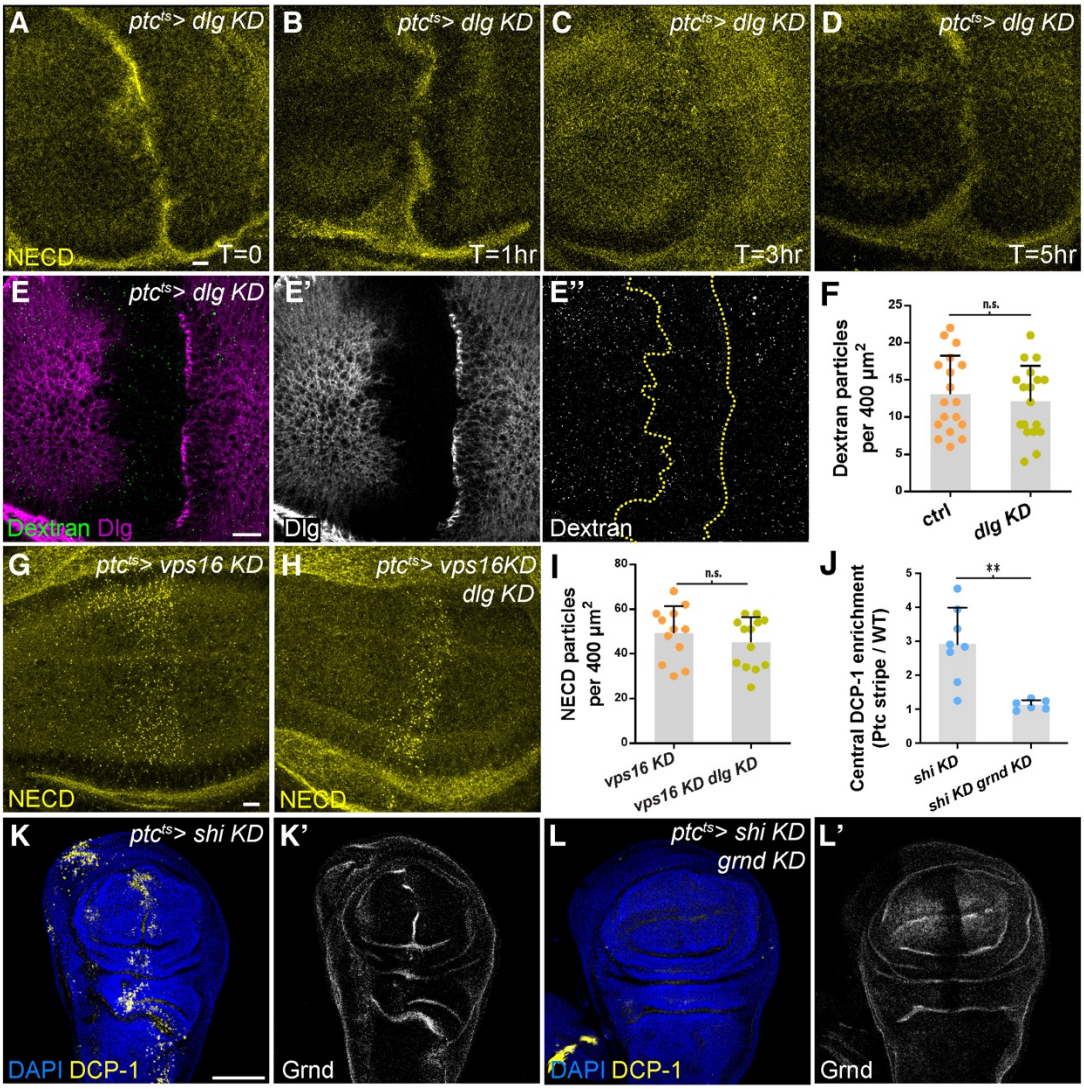
A
ptc^ts> dlg KD
NECD
T=0
B
ptc^ts> dlg KD
T=1hr
C
ptc^ts> dlg KD
T=3hr
D
ptc^ts> dlg KD
T=5hr
E
ptc^ts> dlg KD
Dextran Dlg
E'
Dlg
E''
Dextran
F
Dextran particles per 400 µm²
n.s.
ctrl
dlg KD
G
ptc^ts> vps16 KD
NECD
H
ptc^ts> vps16KD dlg KD
NECD
I
NECD particles per 400 µm²
n.s.
vps16 KD
vps16 KD dlg KD
J
Central DCP-1 enrichment (Ptc stripe / WT)
**
shi KD
shi KD grnd KD
K
ptc^ts> shi KD
DAPI DCP-1
K'
Grnd
L
ptc^ts> shi KD grnd KD
DAPI DCP-1
L'
Grnd

Figure S4

Fig. S4 Polarity-deficient cell elimination does not require endocytosis

Egr signaling in *scrib* cells has been suggested to be driven by increased endocytosis (*12*), but we could not detect changes in endocytic rates of *dlg*-depleted cells, paralleling published work that did not detect endocytic changes in *scrib* or *lgl* cells (*32*).

(A-D): Live trafficking assay shows that Notch (anti-Notch extracellular domain staining) is internalized and degraded in both WT and *dlg*-depleted cells. T=# of hours post-labelling.

(E-F): Endocytic internalization of Dextran is equivalent in WT and *dlg*-depleted cells (**E**), quantitated in **F**.

(G-I): Endocytic Notch accumulation in cells depleted of the lysosomal entry regulator *vps16* to prevent cargo degradation (**G**). No enhancement of Notch accumulation is seen in *dlg* co-depleted cells (**H**), quantitated in **I**.

(J-L): Endocytosis-defective cells depleted of the fly Dynamin, *shibire,* like those depleted of *Rab5* (*33*), undergo Grnd-dependent apoptosis within an otherwise WT wing disc (**K, L**), demonstrating that endocytosis of Grnd is not required for cell elimination, quantitated in **J**. DAPI indicates nuclei, DCP-1 indicates apoptotic cells.

Scale bars: 10 μm in **A, E,** and **G**, 100 μm in **K**.

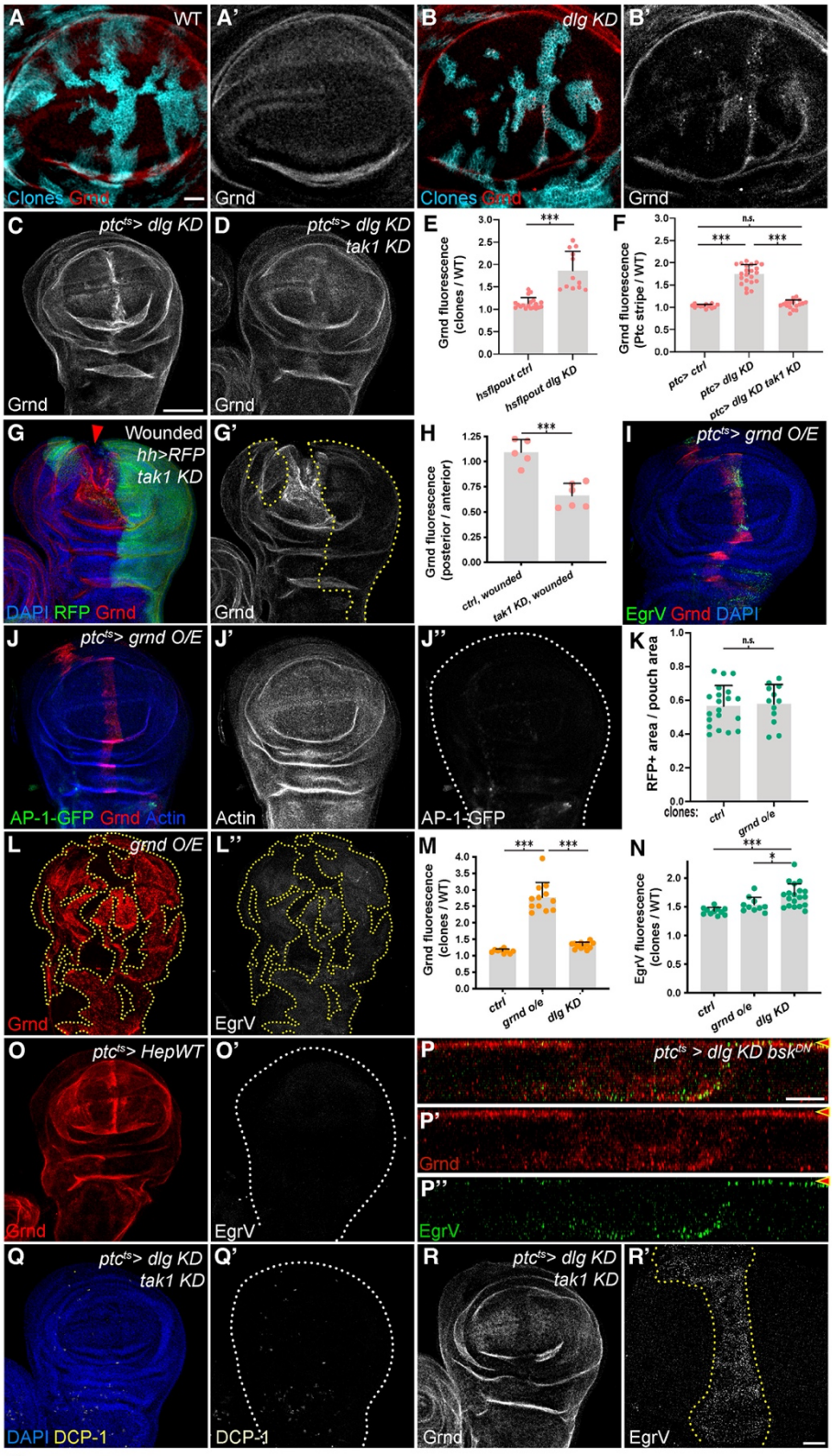
A
WT
Clones Grnd
A'
Grnd
B
dlg KD
Clones Grnd
B'
Grnd
C
ptc^ts> dlg KD
Grnd
D
ptc^ts> dlg KD
tak1 KD
Grnd
E
Grnd fluorescence (clones / WT)
***
hsflpout ctrl
hsflpout dlg KD
F
Grnd fluorescence (Ptc stripe / WT)
n.s.
***
***
ptc> ctrl
ptc> dlg KD
ptc> dlg KD tak1 KD
G
Wounded
hh>RFP
tak1 KD
DAPI RFP Grnd
G'
Grnd
H
Grnd fluorescence (posterior / anterior)
***
ctrl, wounded
tak1 KD, wounded
I
ptc^ts> grnd O/E
EgrV Grnd DAPI
J
ptc^ts> grnd O/E
AP-1-GFP Grnd Actin
J'
Actin
J''
AP-1-GFP
K
RFP+ area / pouch area
n.s.
clones:
ctrl
grnd o/e
L
grnd O/E
Grnd
L''
EgrV
M
Grnd fluorescence (clones / WT)
***
***
ctrl
grnd o/e
dlg KD
N
EgrV fluorescence (clones / WT)
***
*
ctrl
grnd o/e
dlg KD
O
ptc^ts> HepWT
Grnd
O'
EgrV
P
ptc^ts > dlg KD bsk^DN
P'
Grnd
P''
EgrV
Q
ptc^ts> dlg KD
tak1 KD
DAPI DCP-1
Q'
DCP-1
R
ptc^ts> dlg KD
tak1 KD
Grnd
R'
EgrV
S
WT dlg WT dlg
- - + +
PNGase F
34kDa-
26kDa-
Grnd-V5

Figure S5

Fig. S5 Grnd upregulation upon JNK signaling does not account for increased Egr binding

Signal activation could be driven by elevated Grnd levels, but Grnd upregulation did not cause apoptosis in *dlg*-depleted cells. N-glycosylation of Grnd can modulate its affinity for Egr (*8*), however we found no evidence for this mechanism in *dlg*-depleted cells.

(A-F): Compared to WT (**A**), *dlg*-depleted cells show increased levels of Grnd (**B**), and upregulation is dependent on TAK1 (**C, D**), quantitated in **E** and **F**.

(G-H): Wounding also induces upregulation of Grnd in a TAK1-dependent manner (**G**), quantitated in **H**. Arrowhead indicates wound site.

(I-N): Grnd overexpression induces some elevated binding of EgrV (**I**), but not JNK activation, disc folding (**J**), or reduction in the size of clones, quantitated in **K**. *dlg*-depleted cells display lower elevation of Grnd (**L**), quantitated in **M**, but nevertheless higher levels of EgrV binding compared to Grnd-overexpressing cells, quantitated in **N**.

(O) Overexpression of the JNK kinase Hep is sufficient to increase Grnd levels and induce the disc fold, but not EgrV binding.

(P) Blocking apoptosis and extrusion in *dlg*-depleted cells (X-Z section) does not alter Grnd mispolarization nor basal EgrV binding.

(Q-R): Apoptosis of *dlg*-depleted cells (DCP-1 staining) is rescued when JNK signaling is blocked (**Q**), but EgrV binding persists (**R**).

(S) Western blot showing indistinguishable molecular weights of transgenic Grnd in WT vs *dlg* cells; PNGase-treated samples show that both are N-glycosylated.

Scale bars: 25 μm in **A**, 100 μm in **C**, 10 μm in **P** and **R'**.

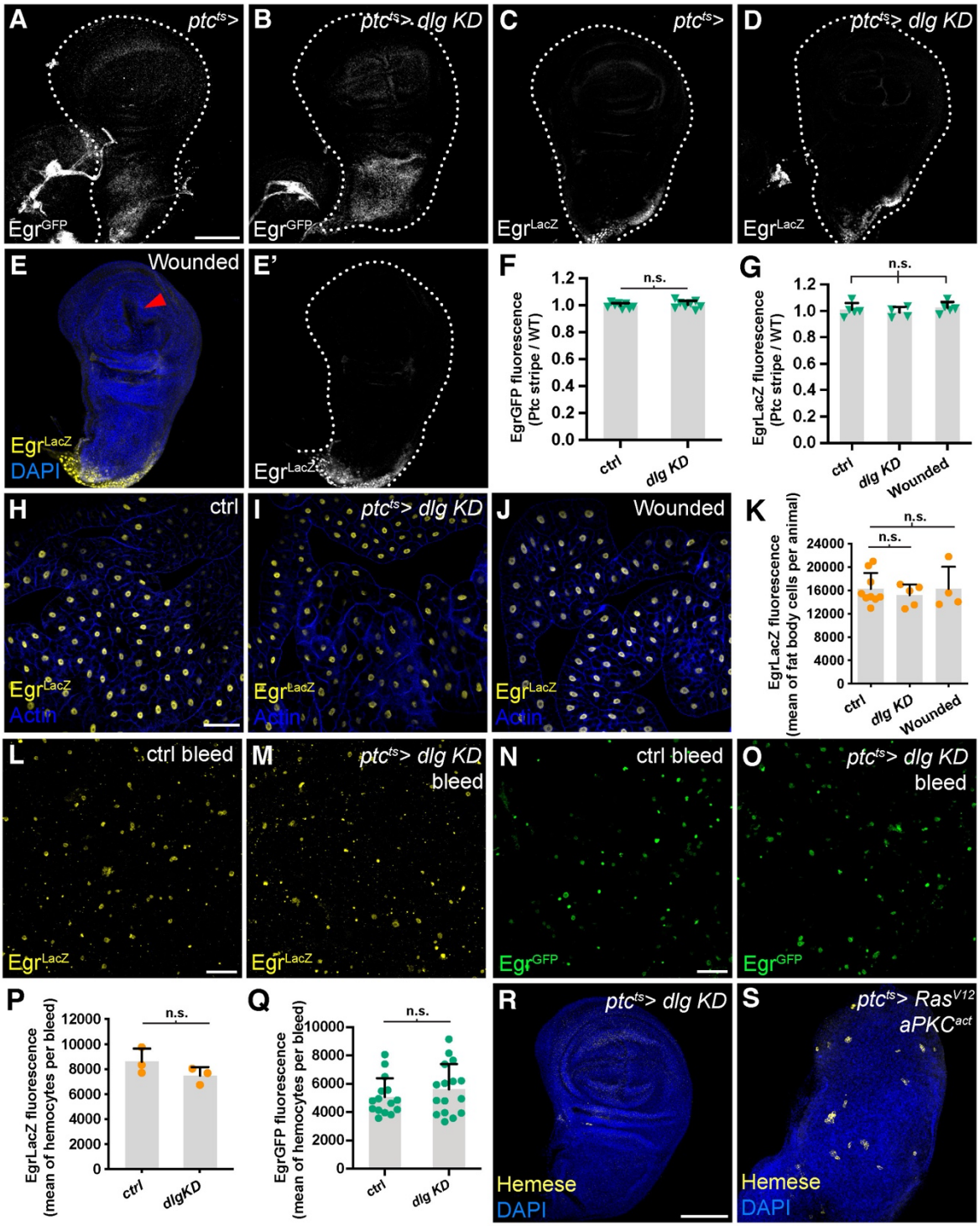
A
ptc^ts>
Egr^GFP
B
ptc^ts> dlg KD
Egr^GFP
C
ptc^ts>
Egr^LacZ
D
ptc^ts> dlg KD
Egr^LacZ
E
Wounded
Egr^LacZ
DAPI
E'
Egr^LacZ
F
EgrGFP fluorescence (Ptc stripe / WT)
n.s.
ctrl
dlg KD
G
EgrLacZ fluorescence (Ptc stripe / WT)
n.s.
ctrl
dlg KD
Wounded
H
ctrl
Egr^LacZ
Actin
I
ptc^ts> dlg KD
Egr^LacZ
Actin
J
Wounded
Egr^LacZ
Actin
K
EgrLacZ fluorescence (mean of fat body cells per animal)
n.s.
n.s.
ctrl
dlg KD
Wounded
L
ctrl bleed
Egr^LacZ
M
ptc^ts> dlg KD bleed
Egr^LacZ
N
ctrl bleed
Egr^GFP
O
ptc^ts> dlg KD bleed
Egr^GFP
P
EgrLacZ fluorescence (mean of hemocytes per bleed)
n.s.
ctrl
dlgKD
Q
EgrGFP fluorescence (mean of hemocytes per bleed)
n.s.
ctrl
dlg KD
R
ptc^ts> dlg KD
Hemese
DAPI
S
ptc^ts> Ras^V12 aPKC^act
Hemese
DAPI

Figure S6

Fig. S6 Egr levels are not elevated during *scrib*-class cell elimination

(A-G): Compared to control (**A**), disc Egr levels, assayed by a GFP-labelled protein trap, are not elevated by *dlg* depletion (**B**), quantitated in **F**. Compared to control (**C**)**,** disc *egr* transcription, assayed by a *lacZ* enhancer trap, is not elevated by *dlg* depletion (**D**) or wounding (**E**), quantitated in **G**.

(H-K) Compared to control (**H**), fat body *egr* transcription is not elevated within larvae undergoing *dlg* cell elimination (**I**) or wounding (**J**), quantitated in **K**.

(L-Q): Compared to control (**L, N**), hemocyte Egr levels, assayed by *lacZ* enhancer trap and GFP-labelled protein trap, are not elevated in larvae undergoing *dlg* cell elimination (**M, O**), quantitated in **P, Q**.

(R-S): Hemocytes do not associate with *dlg*-depleted cells undergoing elimination (**R**). A large tumor driven by overexpression of $aPKC^{act}$+Ras^{act} is shown as a positive control (**S**).

Scale bars: 100 μm in **A** and **R**, 50 μm in **H, L** and **N**.

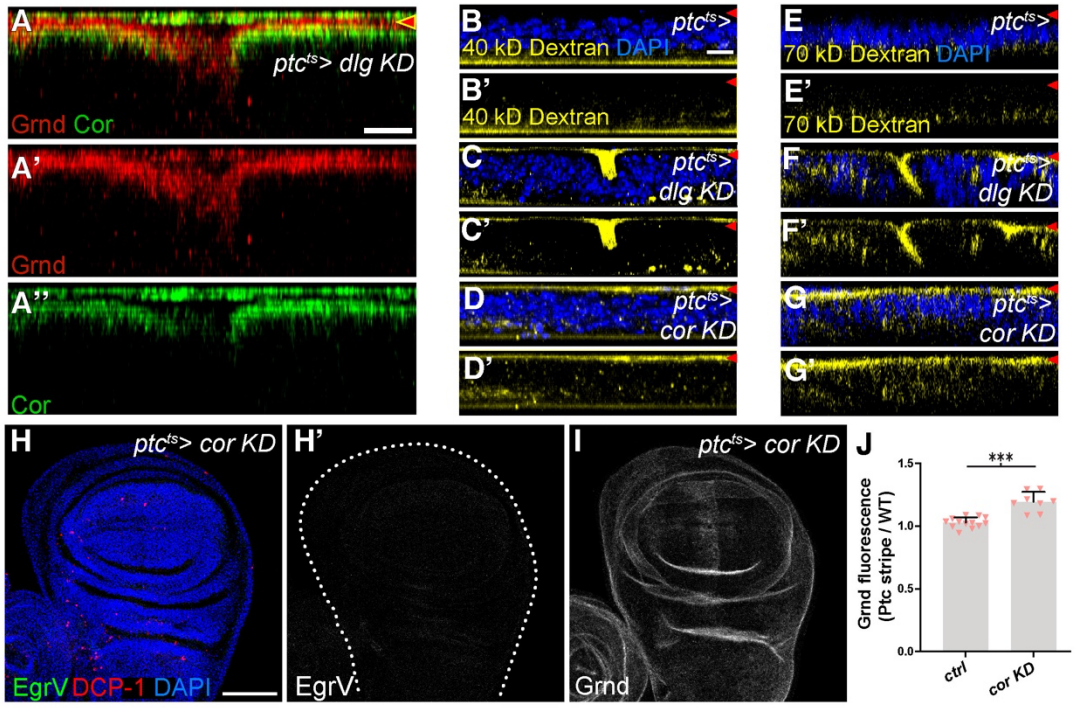
A
ptc^ts> dlg KD
Grnd Cor
A'
Grnd
A''
Cor
B
ptc^ts>
40 kD Dextran DAPI
B'
40 kD Dextran
C
ptc^ts>
dlg KD
C'
D
ptc^ts>
cor KD
D'
E
ptc^ts>
70 kD Dextran DAPI
E'
70 kD Dextran
F
ptc^ts>
dlg KD
F'
G
ptc^ts>
cor KD
G'
H
ptc^ts> cor KD
EgrV DCP-1 DAPI
H'
EgrV
I
ptc^ts> cor KD
Grnd
J
***
Grnd fluorescence
(Ptc stripe / WT)
1.5
1.0
0.5
0.0
ctrl
cor KD

Figure S7

Fig. S7 Epithelial permeability changes do not induce Egr binding or cell elimination

Components of the paracellular barrier are downregulated in *dlg*-depleted cells (*34*), and depletion of one barrier component alone was sufficient to allow luminal Dextran access. However, elevated Egr binding was not seen, nor were cells eliminated. These data suggest that a feature distinct from paracellular permeability is altered to trigger the Egr-Grnd-JNK axis.

(A-G): X-Z sections through wing pouch. Location of lumen is indicated by red arrowheads.

(A): *dlg*-depleted cells lose localization of the septate junction component Cor.

(B-G): *dlg* depletion (**C, F**) as well as *cor* depletion (**D, G**) renders the epithelium permeable to 40kD and 70kD Dextran (compare to control in **B** and **E**).

(H-J): *cor*-depleted cells show a mild elevation of Grnd (**I**), quantitated in **J**, but no EgrV binding nor cell death (**H**).

Scale bars: 10 μm in **A** and **B**, 100 μm in **H**.

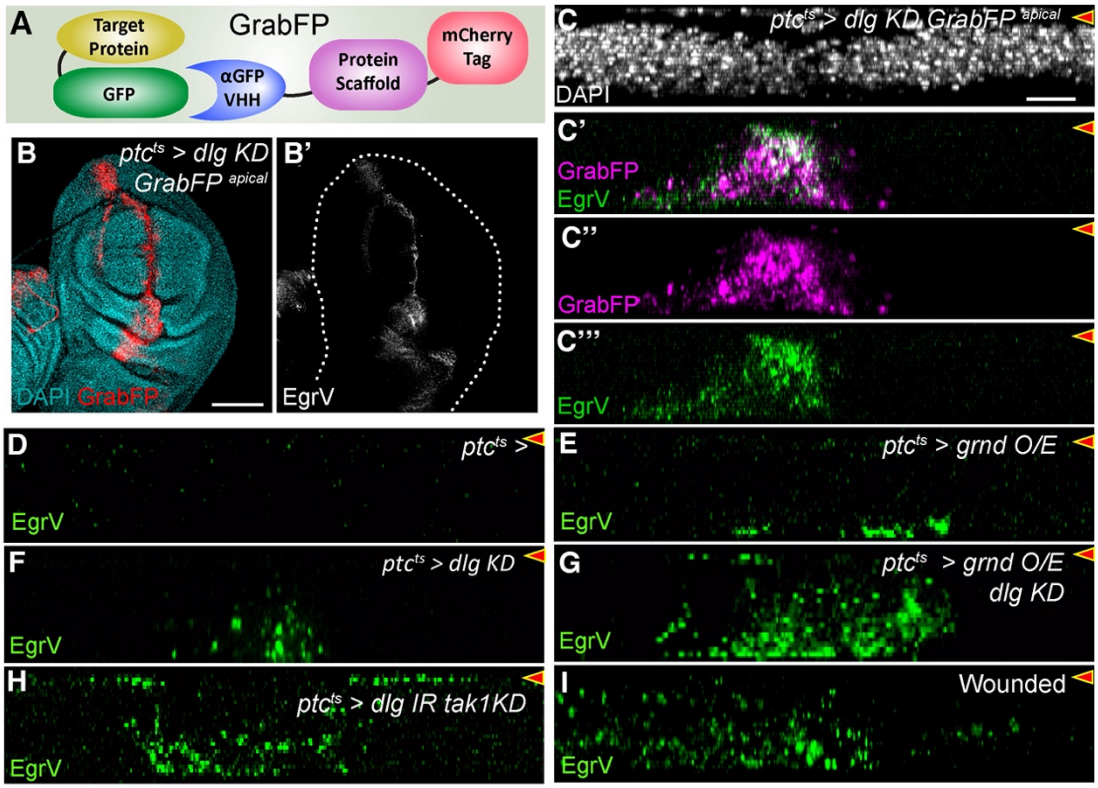
A
Target Protein
GrabFP
mCherry Tag
GFP
αGFP VHH
Protein Scaffold
B
ptc^ts > dlg KD GrabFP apical
DAPI GrabFP
B'
EgrV
C
ptc^ts > dlg KD GrabFP apical
DAPI
C'
GrabFP
EgrV
C''
GrabFP
C'''
EgrV
D
ptc^ts >
EgrV
E
ptc^ts > grnd O/E
EgrV
F
ptc^ts > dlg KD
EgrV
G
ptc^ts > grnd O/E
dlg KD
EgrV
H
ptc^ts > dlg IR tak1KD
EgrV
I
Wounded
EgrV

Figure S8

Fig. S8 Additional data concerning Egr binding in combination with GrabFP and Grnd O/E

(A): In the GrabFP system (*18*), GFP-binding nanobodies are fused to the extracellular domain of proteins targeted to apical or basolateral surfaces.

(B): An apically expressed GFP nanobody is mislocalized basolaterally in the *dlg*-depleted stripe of cells, where it can bind to basolateral EgrV.

(C): X-Z cross-section of disc with genotype in **C**, with disc proper below and peripodium above. Lumen is indicated by red arrowheads.

(D-E): X-Z cross-sections. Compared to control (**D**), Grnd overexpression in the stripe (**E**) allows EgrV to bind basolaterally. Corresponds to **Fig. 3B, C**.

(F-I): X-Z cross-sections. Dlg-depleted cells bind EgrV (**F**) and Grnd overexpression enhances this binding (**G**). Similarly, co-depletion of Tak1 and Dlg (**H**) as well as wounding (**I**) allows basolateral EgrV binding. Corresponds to **Fig. 4A-D**.

Scale bars: 100 μm in **B**, and 10 μm in **C**.

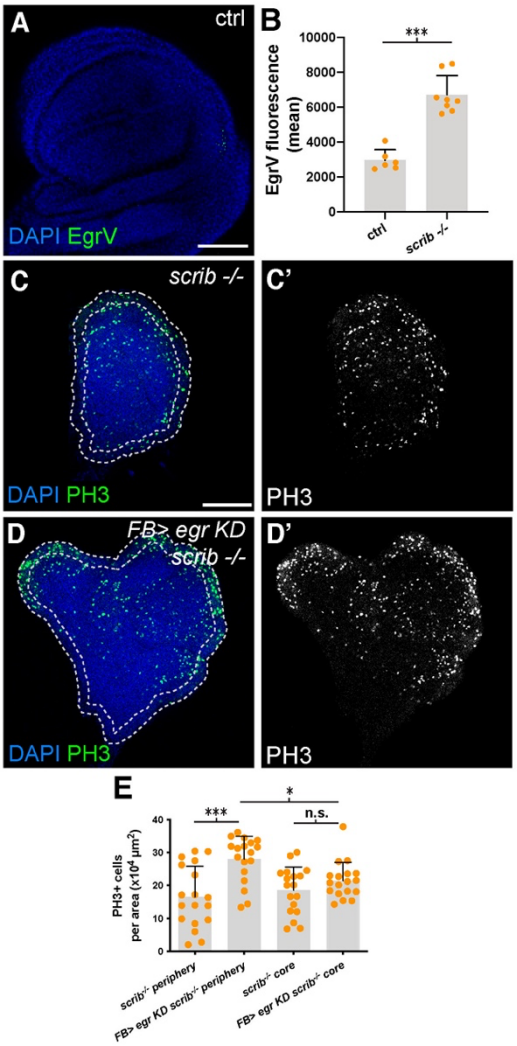
A
ctrl
DAPI EgrV
B
***
EgrV fluorescence (mean)
10000
8000
6000
4000
2000
0
ctrl
scrib -/-
C
scrib -/-
DAPI PH3
C'
PH3
D
FB> egr KD
scrib -/-
DAPI PH3
D'
PH3
E
***
*
n.s.
PH3+ cells per area (x10⁴ µm²)
40
30
20
10
0
scrib-/- periphery
FB> egr KD scrib-/- periphery
scrib-/- core
FB> egr KD scrib-/- core

Figure S9

Fig. S9 Additional data concerning homotypic interactions of polarity-deficient cells

(A-B): Control **(A)** and quantitation **(B)** for Egr binding to discs containing cells of only a single genotype.

(C-E): Depression of mitotic cell frequency in the periphery of *scrib* discs **(C)** is dependent on circulating Egr **(D)**, quantitated in **E**. As with JNK signaling (**Fig. 4F-H**) and apoptosis (**Fig. 4J-L**), circulating Egr does not affect phenotypes in the tissue core.

Scale bars: 50 μm in **A**, and 100 μm in **C**.

SUPPLEMENTAL TABLES

Supplemental Table 1 – Key Resources

Reagent or Resource		**Source**	**Identifier**
Antibodies	**Concentration**		
Mouse anti-Grnd	1:500	Bilder lab	7D9
Rabbit anti-DCP-1	1:300	Cell signaling	9568
Rabbit anti-PH3	1:300	Cell signaling	9701
Mouse anti-NECD	1:25	DSHB	C458.2H
Rb anti-β-gal	1:1000	Abcam	AB616
Rb anti-GFP	1:500	Torrey Pines	TP401
Mouse anti-V5	1:500	Invitrogen	2F11F7
Mouse anti-Hemese	1:100	Ando lab	H2
Mouse anti-Cor	1:500	DSHB	C566.9
Mouse anti-Dlg	1:100	DSHB	4F3
Chemicals			
Phalloidin-TRITC	1:500	Sigma	P1951
DAPI	1:1000	Sigma	D9542
3kD Dextran	1mg/ml	ThermoFisher	D3306
40kD Dextran	1mg/ml	ThermoFisher	D1845
70kD Dextran	1mg/ml	ThermoFisher	D1823

Fly Stocks	**Source**
5xQEDSRed	Zecca and Struhl. 2007 (*27*)
scrib^{1}	Zeitler et al. 2004 (*29*)
scrib^{2}	Zeitler et al. 2004 (*29*)
egr^{1}	Igaki et al. 2002 (*23*)
egr^{3}	Igaki et al. 2002 (*23*)
Egr-LacZ	Muzzopappa et al. 2017 (*16*)
UAS-Egr-venus	Parisi et al. 2014 (*14*)
AP-1-GFP	Chatterjee and Bohmann 2012 (*25*)
AP-1-RFP	Chatterjee and Bohmann 2012 (*25*)
Tub> Myc y+ >Gal4	De La Cova et al. 2004 (*28*)
UAS-Grnd-V5	De Vreede et al. 2018 (*8*)
Uas-aPKC^{Act}	Betschinger et al. 2003 (*26*)
UAS-Egr RNAi on III (45252)	Vienna Drosophila RNAi Center
UAS-Grnd RNAi on II (104538)	Vienna Drosophila RNAi Center
UAS-dlg RNAi on III (41136)	Vienna Drosophila RNAi Center
UAS-Tak1 RNAi on II (101357)	Vienna Drosophila RNAi Center
UAS-Egr RNAi on II (55276)	Bloomington Drosophila Stock Center
UAS-dlg RNAi on II (39035)	Bloomington Drosophila Stock Center
UAS-Shi RNAi on III (36921)	Bloomington Drosophila Stock Center

UAS-Vps16 RNAi on II (38271)	Bloomington Drosophila Stock Center
UAS-Cor RNAi on III (35003)	Bloomington Drosophila Stock Center
UAS-Wgn RNAi on III (50594)	Bloomington Drosophila Stock Center
hsFLP; Act>CD2>Gal4 UAS-RFP/S-T	Bloomington Drosophila Stock Center
FRT82	Bloomington Drosophila Stock Center
UbiGFP	Bloomington Drosophila Stock Center
UbiNLSRFP	Bloomington Drosophila Stock Center
Egr-GFSTF	Bloomington Drosophila Stock Center
En-Gal4	Bloomington Drosophila Stock Center
R4-Gal4	Bloomington Drosophila Stock Center
CG-Gal4	Bloomington Drosophila Stock Center
HmlΔ-Gal4	Bloomington Drosophila Stock Center
Hh-Gal4	Bloomington Drosophila Stock Center
Ptc-Gal4	Bloomington Drosophila Stock Center
Nub-Gal4	Bloomington Drosophila Stock Center
Ppl-Gal4	Bloomington Drosophila Stock Center
MS1096-Gal4	Bloomington Drosophila Stock Center
Tub-Gal4	Bloomington Drosophila Stock Center
Act-Gal4	Bloomington Drosophila Stock Center
hsFLP^{122}	Bloomington Drosophila Stock Center

UAS-hisRFP	Bloomington Drosophila Stock Center
UAS-GFP	Bloomington Drosophila Stock Center
yw	Bloomington Drosophila Stock Center
Tub-Gal80TS	Bloomington Drosophila Stock Center
UAS-GrabFP-Vkg-mCherry	Bloomington Drosophila Stock Center
UAS-GrabFP-ApicalExt-mCherry	Bloomington Drosophila Stock Center
UAS-Hep^{WT}	Bloomington Drosophila Stock Center
UAS-Ras^{v12}	Bloomington Drosophila Stock Center
UAS-bsk^{DN}	Bloomington Drosophila Stock Center

Supplemental Table 2 – Detailed Genotypes

Figure	Panel	Genotype
1	B	*hsFLP; Act>CD2>Gal4 UAS RFP/+*
	C	*hsFLP; Act>CD2>Gal4 UAS RFP/+; UAS-Dlg RNAi/+*
	D	*hsFLP; Act>CD2>Gal4 UAS RFP/UAS-Grnd RNAi; UAS-Dlg RNAi/+*
	G	*Ptc-Gal4 Tub-Gal80TS/+*
	H	*Ptc-Gal4 Tub-Gal80TS/+; UAS-Dlg RNAi/+*
	I	*Ptc-Gal4 Tub-Gal80TS/+*
	J	*Ptc-Gal4 Tub-Gal80TS/+; UAS-Dlg RNAi/+*
	K	*Ptc-Gal4 Tub-Gal80TS/UAS-Grnd RNAi; UAS-Dlg RNAi/+*
2	A	*Ptc-Gal4 Tub-Gal80TS/+; UAS-Dlg RNAi/UAS Egr RNAi*
	B	*Ptc-Gal4 Tub-Gal80TS/HmlΔ-Gal4; UAS-Dlg RNAi/UAS Egr RNAi*
	C	*Ptc-Gal4 Tub-Gal80TS/R4-Gal4; UAS-Dlg RNAi/UAS Egr RNAi*
	E	*hsFLP;; UbiNLSRFP FRT82B/FRT82B*
	F	*hsFLP;; UbiNLSRFP FRT82B/scrib^{2} FRT82B*
	G	*hsFLP; egr^{1}/egr^{3}; UbiNLSRFP FRT82B/ scrib^{2} FRT82B*
	H	*hsFLP; en-Gal4 UAS-GFP/UAS Egr RNAi; UbiNLSRFP FRT82B/ scrib^{2} FRT82B*
	I	*hsFLP; en-Gal4 UAS-GFP/UAS Grnd RNAi; UbiNLSRFP FRT82B/ scrib^{2} FRT82B*
	J	*hsFLP; CG-Gal4/UAS Egr RNAi; UbiNLSRFP FRT82B/ scrib^{2} FRT82B*
	K	*hsFLP; HmlΔ-Gal4/UAS Egr RNAi; UbiNLSRFP FRT82B/ scrib^{2} FRT82B*

3	**B**	*Ptc-Gal4 Tub-Gal80TS/+*
	C	*Ptc-Gal4 Tub-Gal80TS/UAS-Grnd-V5*
	D	*5xQEDSred/+*
	E	*5xQEDSred/+*
	F	*UAS-GrabFP-Vkg-mCherry/+; R4-Gal4/+*
	G	*MS1096-Gal4/+;; UAS-GrabFP-ApicalExt-mCherry/+*
	H	*MS1096-Gal4/+;; UAS-GrabFP-ApicalExt-mCherry/+*
4	**A**	*Ptc-Gal4 Tub-Gal80TS/+; UAS-Dlg RNAi/+*
	B	*Ptc-Gal4 Tub-Gal80TS/UAS-Grnd-V5; UAS-Dlg RNAi/+*
	C	*Ptc-Gal4 Tub-Gal80TS/UAS-Tak1 RNAi; UAS-Dlg RNAi/+*
	D	*5xQEDSred/+*
	E	$scrib^{1}/scrib^{2}$
	F	*ppl-Gal4/+;* $scrib^{1}$*, AP-1-RFP/*$scrib^{2}$
	G	*ppl-Gal4/UAS-egr RNAi;* $scrib^{1}$*, AP-1-RFP/*$scrib^{2}$
	J	*ppl-Gal4/+;* $scrib^{1}/scrib^{2}$
	K	*ppl-Gal4/UAS-egr RNAi;* $scrib^{1}/scrib^{2}$
S1	**A**	*hsFLP; Act>CD2>Gal4 UAS RFP/+*
	B	*hsFLP; Act>CD2>Gal4 UAS RFP/+; UAS-Dlg RNAi/+*
	C	*hsFLP; Act>CD2>Gal4 UAS RFP/UAS-Grnd RNAi; UAS-Dlg RNAi/+*
	D	*Ptc-Gal4 Tub-Gal80TS/+*

	E	*Ptc-Gal4 Tub-Gal80TS/+; UAS-Dlg RNAi/+*
	G	*hsFLP;; UbiNLSRFP FRT82B/scrib^{2} FRT82B*
	H	*hsFLP; Uas RedStinger/+; Tub>myc y+>Gal4/+*
	K	*hsFLP; Act>CD2>Gal4 UAS RFP/+; UAS-Dlg RNAi/+*
S2	**A**	*AP-1-GFP/+; Hh-Gal4 UAS-CD8RFP/+*
	B	*AP-1-GFP/UAS-Grnd RNAi; Hh-Gal4 UAS-CD8RFP/+*
	C	*UAS-Egr-venus/+; R4-Gal4/+*
	D	*UAS-Egr-venus/5xQEDSRed; R4-Gal4/+*
	G	*yw*
	I	*UAS-Grnd RNAi/+; Hh-Gal4 UAS-CD8RFP/+*
S3	**A**	*Ptc-Gal4 Tub-Gal80TS/UAS-GFP*
	B	*Ptc-Gal4 Tub-Gal80TS/UAS-GFP ; UAS-Dlg RNAi/+*
	C	*Ptc-Gal4 Tub-Gal80TS/+; UAS-Dlg RNAi/+*
	D	*Ptc-Gal4 Tub-Gal80TS/+; UAS-Dlg RNAi/UAS-Wgn RNAi*
	F	*Ptc-Gal4 Tub-Gal80TS/+; UAS-Dlg RNAi/UAS Egr RNAi*
	G	*Ptc-Gal4 Tub-Gal80TS/HmlΔ-Gal4; UAS-Dlg RNAi/UAS Egr RNAi*
	H	*Ptc-Gal4 Tub-Gal80TS/R4-Gal4; UAS-Dlg RNAi/UAS Egr RNAi*
S4	**A**	*Ptc-Gal4 Tub-Gal80TS/+; UAS-Dlg RNAi/+*
	B	*Ptc-Gal4 Tub-Gal80TS/+; UAS-Dlg RNAi/+*
	C	*Ptc-Gal4 Tub-Gal80TS/+; UAS-Dlg RNAi/+*

	D	*Ptc-Gal4 Tub-Gal80TS/+; UAS-Dlg RNAi/+*
	E	*Ptc-Gal4 Tub-Gal80TS/+; UAS-Dlg RNAi/+*
	G	*Ptc-Gal4 Tub-Gal80TS/UAS-Vps16 RNAi*
	H	*Ptc-Gal4 Tub-Gal80TS/UAS-Vps16 RNAi; UAS-Dlg RNAi/ +*
	K	*Ptc-Gal4 Tub-Gal80TS/+; UAS-Shi RNAi/+*
	L	*Ptc-Gal4 Tub-Gal80TS/UAS-Grnd RNAi; UAS-Shi RNAi/+*
S5	**A**	*hsFLP; Act>CD2>Gal4 UAS RFP/+*
	B	*hsFLP; Act>CD2>Gal4 UAS RFP/+; UAS-Dlg RNAi/+*
	C	*Ptc-Gal4 Tub-Gal80TS/+; UAS-Dlg RNAi/+*
	D	*Ptc-Gal4 Tub-Gal80TS/UAS-Tak1 RNAi; UAS-Dlg RNAi/+*
	G	*Hh-Gal4 UAS-CD8RFP/UAS-Tak1 RNAi*
	I	*Ptc-Gal4 Tub-Gal80TS/UAS-Grnd-V5*
	J	*Ptc-Gal4 Tub-Gal80TS/UAS-Grnd-V5; AP-1-GFP/+*
	L	*hsFLP; Act>CD2>Gal4 UAS RFP/UAS-Grnd-V5*
	O	*Ptc-Gal4 Tub-Gal80TS/UAS-HepWT*
	P	*Ptc-Gal4 Tub-Gal80TS/+; UAS-Dlg RNAi/UAS-Bsk^{DN}*
	Q	*Ptc-Gal4 Tub-Gal80TS/UAS-Tak1 RNAi; UAS-Dlg RNAi/+*
	R	*Ptc-Gal4 Tub-Gal80TS/UAS-Tak1 RNAi; UAS-Dlg RNAi/+*
S6	**A**	*Ptc-Gal4 Tub-Gal80TS/Egr-GFP*
	B	*Ptc-Gal4 Tub-Gal80TS/Egr-GFP; UAS-Dlg RNAi/+*

	C	*Ptc-Gal4 Tub-Gal80TS/+; Egr-LacZ/+*
	D	*Ptc-Gal4 Tub-Gal80TS/+; UAS-Dlg RNAi/ Egr-LacZ*
	E	*5xQEDSred/+; Egr-LacZ/+*
	H	*Ptc-Gal4 Tub-Gal80TS/+; Egr-LacZ/+*
	I	*Ptc-Gal4 Tub-Gal80TS/+; UAS-Dlg RNAi/ Egr-LacZ*
	J	*5xQEDSred/+; Egr-LacZ/+*
	L	*Ptc-Gal4 Tub-Gal80TS/+; Egr-LacZ/+*
	M	*Ptc-Gal4 Tub-Gal80TS/+; UAS-Dlg RNAi/ Egr-LacZ*
	N	*Ptc-Gal4 Tub-Gal80TS/Egr-GFP*
	O	*Ptc-Gal4 Tub-Gal80TS/Egr-GFP; UAS-Dlg RNAi/+*
	R	*Ptc-Gal4 Tub-Gal80TS/+; UAS-Dlg RNAi/+*
	S	*Ptc-Gal4 Tub-Gal80TS/UAS-Ras^{V12}; UAS-aPKC^{act}/+*
S7	**A**	*Ptc-Gal4 Tub-Gal80TS/+; UAS-Dlg RNAi/+*
	B	*Ptc-Gal4 Tub-Gal80TS/+*
	C	*Ptc-Gal4 Tub-Gal80TS/+; UAS-Dlg RNAi/+*
	D	*Ptc-Gal4 Tub-Gal80TS/+; UAS-Cor RNAi/+*
	E	*Ptc-Gal4 Tub-Gal80TS/+*
	F	*Ptc-Gal4 Tub-Gal80TS/+; UAS-Dlg RNAi/+*
	G	*Ptc-Gal4 Tub-Gal80TS/+; UAS-Cor RNAi/+*
	H	*Ptc-Gal4 Tub-Gal80TS/+; UAS-Cor RNAi/+*

	I	*Ptc-Gal4 Tub-Gal80TS/+; UAS-Cor RNAi/+*
S8	**B**	*Ptc-Gal4 Tub-Gal80TS/+; UAS-Dlg RNAi/UAS-GrabFP-ApicalExt-mCherry*
	C	*Ptc-Gal4 Tub-Gal80TS/+; UAS-Dlg RNAi/UAS-GrabFP-ApicalExt-mCherry*
	D	*Ptc-Gal4 Tub-Gal80TS/+*
	E	*Ptc-Gal4 Tub-Gal80TS/UAS-Grnd-V5*
	F	*Ptc-Gal4 Tub-Gal80TS/+; UAS-Dlg RNAi/+*
	G	*Ptc-Gal4 Tub-Gal80TS/UAS-Grnd-V5; UAS-Dlg RNAi/+*
	H	*Ptc-Gal4 Tub-Gal80TS/UAS-Tak1 RNAi; UAS-Dlg RNAi/+*
	I	*5xQEDSred/+*
S9	**A**	*yw*
	C	*ppl-Gal4/+; scrib^{1}/scrib^{2}*
	D	*ppl-Gal4/UAS-egr RNAi; scrib^{1}/scrib^{2}*

Supplemental Table 3 – Statistical Tests

<table>
<tr><th>Figure</th><th>Panel</th><th>Statistical test</th></tr>
<tr><td rowspan="2">1</td><td>E</td><td>EgrV fluorescence (clones / WT); Individual units: Wing discs; n=11 for ctrl, n=19 for dlg KD, n=19 for dlg KD grnd KD; Values: Ratio of mean fluorescence measurements of cells in the wing pouch on 16-bit images; Ordinary one-way ANOVA test, Tukey’s multiple comparisons; P<0.0001; F=23.33; DF=48
<table>
<tr><td>Multiple comparisons</td><td>P value</td></tr>
<tr><td>ctrl vs. dlg KD</td><td><0.0001</td></tr>
<tr><td>ctrl vs. dlg KD grnd KD</td><td>0.5958</td></tr>
<tr><td>dlg KD vs. dlg KD grnd KD</td><td><0.0001</td></tr>
</table></td></tr>
<tr><td>F</td><td>RFP+ area / pouch area; Individual units: Wing discs; n=20 for ctrl, n=19 for dlg KD, n=19 for dlg KD grnd KD; Values: Ratio of area measurements of cells in the wing pouch; Ordinary one-way ANOVA test, Tukey’s multiple comparisons; P<0.0001; F=80.06; DF=57
<table>
<tr><td>Multiple comparisons</td><td>P value</td></tr>
<tr><td>ctrl vs. dlg KD</td><td><0.0001</td></tr>
<tr><td>ctrl vs. dlg KD grnd KD</td><td>0.1777</td></tr>
<tr><td>dlg KD vs. dlg KD grnd KD</td><td><0.0001</td></tr>
</table></td></tr>
</table>

<table>
<tr>
<td></td>
<td>L</td>
<td>EgrV fluorescence (Ptc stripe / WT); Individual units: Wing discs; n=14 for ctrl, n=31 for dlg KD, n=15 for dlg KD grnd KD; Values: Ratio of mean fluorescence measurements of cells in the wing pouch on 16-bit images; Ordinary one-way ANOVA test, Tukey’s multiple comparisons; P<0.0001; F=14.41; DF=59
<table>
<tr><td>Multiple comparisons</td><td>P value</td></tr>
<tr><td>ctrl vs. dlg KD</td><td>0.0001</td></tr>
<tr><td>ctrl vs. dlg KD grnd KD</td><td>0.9880</td></tr>
<tr><td>dlg KD vs. dlg KD grnd KD</td><td>0.0002</td></tr>
</table>
</td>
</tr>
<tr>
<td>2</td>
<td>D</td>
<td>Central DCP-1 enrichment (Ptc stripe / WT); Individual units: Wing discs; n=11 for ctrl, n=11 for ptc> dlg KD ctrl, n=10 for ptc> dlg KD grnd KD, n=11 for ptc> dlg KD egr KD, n=12 for hem+ptc> dlg KD egr KD, n=12 for FB+ptc> dlg KD egr KD; Values: Ratio of mean fluorescence measurements of cells in the wing pouch on 16-bit images; Ordinary one-way ANOVA test, Tukey’s multiple comparisons; P<0.0001; F=22.90; DF=66
<table>
<tr><td>Multiple comparisons</td><td>P value</td></tr>
<tr><td>ctrl vs. ptc>dlg KD</td><td><0.0001</td></tr>
<tr><td>ptc> dlg KD vs. ptc>dlg KD grnd KD</td><td><0.0001</td></tr>
<tr><td>ptc> dlg KD vs. ptc> dlg KD egr KD</td><td>0.9997</td></tr>
<tr><td>ptc> dlg KD vs. hem+ptc> dlg KD egr KD</td><td>>0.9999</td></tr>
<tr><td>ptc> dlg KD vs. FB+ptc> dlg KD egr KD</td><td><0.0001</td></tr>
</table>
</td>
</tr>
</table>

L

RFP- / sibling RFP+ clone area; Individual units: Wing discs; n=18 for ctrl, n=19 for scrib ctrl, n=22 for hem> egr KD, n=12 for en> egr KD, n=8 for en> grnd KD, n=15 for FB+hem> egr KD, n=6 for egr null; Values: Ratio of area measurements of cells in the wing pouch; Ordinary one-way ANOVA test, Tukey's multiple comparisons; P<0.0001; F=149.9; DF=99

Multiple comparisons	P value
ctrl vs. scrib ctrl	<0.0001
ctrl vs. hem> egr KD	<0.0001
ctrl vs. en> egr KD	<0.0001
ctrl vs. en> grnd KD	0.0006
ctrl vs. FB+hem> egr KD	<0.0001
ctrl vs. egr null	<0.0001
scrib ctrl vs. hem> egr KD	0.9991
scrib ctrl vs. en> egr KD	0.9995
hem> egr KD vs. en> egr KD	>0.9999
hem> egr KD vs. en> grnd KD	<0.0001
hem> egr KD vs. FB+hem> egr KD	<0.0001
hem> egr KD vs. egr null	<0.0001
en> grnd KD vs. FB+hem> egr KD	<0.0001
en> grnd KD vs. egr null	<0.0001
FB+hem> egr KD vs. egr null	0.0099

<table>
<tr>
<td>4</td>
<td>H</td>
<td>AP-1-RFP fluorescence (mean); Individual units: Peripheral and core tissue regions of wing disc tumors; n=10 for scrib-/- periphery, n=10 for scrib-/- core, n=10 for FB> egr KD scrib-/- periphery, n=10 for FB> egr KD scrib-/- core; Values: Mean fluorescence measurements of cells in the tumor periphery or core on 16-bit images; Ordinary one-way ANOVA test, Tukey’s multiple comparisons; P<0.0001; F=25.50; DF=39
<table>
<tr><td>Multiple comparisons</td><td>P value</td></tr>
<tr><td>scrib-/- periphery vs. FB> egr KD scrib-/- periphery</td><td><0.0001</td></tr>
<tr><td>FB> egr KD scrib-/- periphery vs. scrib-/- core</td><td>0.8726</td></tr>
<tr><td>FB> egr KD scrib-/- periphery vs.
FB> egr KD scrib-/- core</td><td>0.1689</td></tr>
<tr><td>scrib-/- core vs. FB> egr KD scrib-/- core</td><td>0.5360</td></tr>
</table>
</td>
</tr>
<tr>
<td></td>
<td>I</td>
<td>Volume; Individual units: Wing discs; n=10 for ctrl, n=12 for scrib-/-, n=13 for FB>egr KD scrib-/-; Values: Volume measurements; Ordinary one-way ANOVA test, Tukey’s multiple comparisons; P<0.0001; F=42.47; DF=34
<table>
<tr><td>Multiple comparisons</td><td>P value</td></tr>
<tr><td>ctrl vs. FB> egr KD scrib-/-</td><td><0.0001</td></tr>
<tr><td>scrib-/- vs. FB> egr KD scrib-/-</td><td><0.0001</td></tr>
</table>
</td>
</tr>
</table>

<table>
<tr>
<td></td>
<td>L</td>
<td>DCP-1 fluorescence (mean); Individual units: Peripheral and core tissue regions of wing disc tumors; n=10 for scrib-/- periphery, n=10 for scrib-/- core, n=10 for FB> egr KD scrib-/- periphery, n=10 for FB> egr KD scrib-/- core; Values: Mean fluorescence measurements of cells in the tumor periphery or core on 16-bit images; Ordinary one-way ANOVA test, Tukey’s multiple comparisons; P<0.0001; F=29.85; DF=39
<table>
<tr><td>Multiple comparisons</td><td>P value</td></tr>
<tr><td>scrib-/- periphery vs. FB> egr KD scrib-/- periphery</td><td><0.0001</td></tr>
<tr><td>FB> egr KD scrib-/- periphery vs. scrib-/- core</td><td>0.4202</td></tr>
<tr><td>FB> egr KD scrib-/- periphery vs.

FB> egr KD scrib-/- core</td><td>0.9425</td></tr>
<tr><td>scrib-/- core vs. FB> egr KD scrib-/- core</td><td>0.7583</td></tr>
</table>
</td>
</tr>
<tr>
<td>S1</td>
<td>F</td>
<td>Ptc stripe size (Ptc stripe / WT); Individual units: Wing discs; n=11 for dlgKD, n=8 for dlgKD grndKD; Values: Ratio of area measurements of cells in the wing pouch; Two-sided Student’s T-test; t=13.26; DF=17
<table>
<tr><td>Comparison</td><td>P value</td></tr>
<tr><td>dlgKD vs. dlgKD grndKD</td><td><0.0001</td></tr>
</table>
</td>
</tr>
</table>

I

EgrV fluorescence (clones / WT); Individual units: Wing discs; n=7 for ctrl, n=10 for scrib; Values: Ratio of mean fluorescence measurements of cells in the wing pouch on 16-bit images; Two-sided Student's T-test; t=2.353; DF=15

Comparison	P value
ctrl vs. scrib	0.0327

J

EgrV fluorescence (mean); Individual units: Wing discs; n=6 for WT, n=6 for Myc O/E; Values: Mean fluorescence measurements of Myc O/E clones or WT cells in the wing pouch on 16-bit images; Two-sided Student's T-test; t=0.4662, DF=10

Comparison	P value
WT vs. Myc O/E	0.6511

L

ANF fluorescence (mean); Individual units: Wing discs; n=7 for ctrl, n=8 for dlg KD; Values: Mean fluorescence measurements of clone cells in the wing pouch on 16-bit images; Two-sided Student's T-test; t=1.155, DF=13

Comparison	P value
ctrl vs. dlg KD	0.2689

<table>
<tr><td>S2</td><td>E</td><td>AP-1-GFP fluorescence (posterior / anterior); Individual units: Wing discs; n=19 for ctrl, n=16 for grnd KD; Values: Ratio of mean fluorescence measurements of cells in the wing pouch on 16-bit images; Two-sided Student’s T-test; t=7.330; DF=33

<table><tr><td>Comparison</td><td>P value</td></tr><tr><td>ctrl vs. grnd KD</td><td><0.0001</td></tr></table></td></tr>
<tr><td></td><td>F</td><td>EgrV fluorescence (mean); Individual units: Wing discs; n=17 for ctrl, n=15 for wounded; Values: Mean fluorescence measurements of cells in the wing pouch on 16-bit images; Two-sided Student’s T-test; t=6.987; DF=30

<table><tr><td>Comparison</td><td>P value</td></tr><tr><td>ctrl vs. wounded</td><td><0.0001</td></tr></table></td></tr>
<tr><td></td><td>H</td><td>Fluorescence (EgrV or ANF as indicated, mean); Individual units: Wing discs; n=17 for ctrl EgrV, n=15 for wounded EgrV, n=8 for ctrl wounded ANF; Values: Mean fluorescence measurements of cells in the wing pouch on 16-bit images; Ordinary one-way ANOVA test, Tukey’s multiple comparisons; P<0.0001; F=40.08; DF=39

<table><tr><td>Multiple comparisons</td><td>P value</td></tr><tr><td>ctrl EgrV vs. wounded EgrV</td><td><0.0001</td></tr><tr><td>ctrl EgrV vs. ctrl wounded ANF</td><td>0.3942</td></tr><tr><td>wounded EgrV vs. ctrl wounded ANF</td><td><0.0001</td></tr></table></td></tr>
</table>

K

Percentage of adult wings (No defect / Mild defect / Severe defect); Individual units: Adult wings; n=138 for nub> ctrl, n=102 for egr KD ctrl, n=72 for FB> egr KD, n=71 for hem> egr KD, n=56 for nub> egr KD, n=77 for nub> grnd KD, n=120 for nub> Bsk-DN; Values: Scored by severity of adult wing defects; Chi-squared test, Bonferroni correction for 7 groups ; n.s. $P>0.05$; * $P\leq0.0024$; ** $P\leq0.00048$; *** $P\leq0.00005$

Comparison	P value
nub> ctrl vs. egr KD ctrl	0.623674
nub> ctrl vs. FB> egr KD	0.001066
nub> ctrl vs. hem> egr KD	0.000015
nub> ctrl vs. nub> egr KD	0.000313
nub> ctrl vs. nub> grnd KD	0.00001
nub> ctrl vs. nub> Bsk-DN	0.00001
FB> egr KD vs. hem> egr KD	0.360268
FB> egr KD vs. nub> egr KD	0.824513
FB> egr KD vs. nub> grnd KD	0.060977
hem> egr KD vs. nub> egr KD	0.529263
hem> egr KD vs. nub> grnd KD	0.047252
nub> egr KD vs. nub> grnd KD	0.255103
nub> grnd KD vs. nub> Bsk-DN	0.021261

<table>
<tr>
<td>S3</td>
<td>E</td>
<td>Central DCP-1 enrichment (Ptc stripe / WT); Individual units: Wing discs; n=11 for ctrl, n=6 for ptc>dlg KD, n=9 for ptc>dlg KD + wgn KD; Values: Ratio of mean fluorescence measurements of cells in the wing pouch on 16-bit images; Ordinary one-way ANOVA test, Tukey’s multiple comparisons; P<0.0001; F=29.51; DF=25
<table>
<tr><td>Multiple comparisons</td><td>P value</td></tr>
<tr><td>ctrl vs. ptc> dlg KD</td><td><0.0001</td></tr>
<tr><td>ctrl vs. ptc> dlg KD + wgn KD</td><td><0.0001</td></tr>
<tr><td>ptc>dlg KD vs. ptc> dlg KD + wgn KD</td><td>0.5722</td></tr>
</table>
</td>
</tr>
<tr>
<td></td>
<td>I</td>
<td>Central DCP-1 enrichment (Ptc stripe / WT); Individual units: Wing discs; n=10 for ptc>+, n=12 for ptc>dlgKD, n=11 for hem+ptc>dlgKD, n=12 for FB+ptc>dlgKD; Values: Ratio of mean fluorescence measurements of cells in the wing pouch on 16-bit images; Ordinary one-way ANOVA test, Tukey’s multiple comparisons; P<0.0001; F=18.60; DF=44
<table>
<tr><td>Multiple comparisons</td><td>P value</td></tr>
<tr><td>ptc>+ vs. ptc>dlgKD</td><td><0.0001</td></tr>
<tr><td>ptc>+ vs. hem+ptc>dlgKD</td><td><0.0001</td></tr>
<tr><td>ptc>+ vs. FB+ptc>dlgKD</td><td><0.0001</td></tr>
<tr><td>ptc>dlgKD vs. hem+ptc>dlgKD</td><td>0.6347</td></tr>
<tr><td>ptc>dlgKD vs. FB+ptc>dlgKD</td><td>0.7760</td></tr>
<tr><td>hem+ptc>dlgKD vs. FB+ptc>dlgKD</td><td>0.9938</td></tr>
</table>
</td>
</tr>
</table>

<table>
<tr>
<td></td>
<td>J</td>
<td>Ptc stripe size (Ptc stripe / WT); Individual units: Wing discs; n=11 for ptc>dlgKD, n=11 for ptc>dlg KD egrKD, n=11 for hem+ptc>dlg KD egrKD, n=8 for FB+ptc>dlgKD egrKD; Values: Ratio of area measurements of cells in the wing pouch; Ordinary one-way ANOVA test, Tukey’s multiple comparisons; P<0.0001; F=49.06; DF=40
<table>
<tr><td>Multiple comparisons</td><td>P value</td></tr>
<tr><td>ptc>dlgKD vs. ptc>dlgKD egrKD</td><td>0.8278</td></tr>
<tr><td>ptc>dlgKD vs. hem+ptc>dlg KD egrKD</td><td>0.7420</td></tr>
<tr><td>ptc>dlgKD vs. FB+ptc>dlgKD egrKD</td><td><0.0001</td></tr>
<tr><td>ptc>dlgKD egrKD vs. hem+ptc>dlg KD egrKD</td><td>0.9985</td></tr>
<tr><td>ptc>dlgKD egrKD vs. FB+ptc>dlgKD egrKD</td><td><0.0001</td></tr>
<tr><td>hem+ptc>dlg KD egrKD vs. FB+ptc>dlgKD egrKD</td><td><0.0001</td></tr>
</table>
</td>
</tr>
<tr>
<td>S4</td>
<td>F</td>
<td>Dextran particles per 400 µM^2; Individual units: Wing discs; n=18 for ctrl, n=18 for dlg KD; Values: Particles counted per 400 µM^2; Two-sided Student’s T-test; t=0.5664; DF=34
<table>
<tr><td>Comparison</td><td>P value</td></tr>
<tr><td>ctrl vs. dlg KD</td><td>0.5748</td></tr>
</table>
</td>
</tr>
</table>

<table>
<tr><td></td><td>I</td><td>NECD particles per 400 μM^2; Individual units: Wing discs; n=12 for vps16 KD, n= 13 for vps16 KD dlg KD; Values: Particles counted per 400 μM^2; Two-sided Student’s T-test; t=0.8757; DF=23

<table><tr><td>Comparison</td><td>P value</td></tr><tr><td>vps16 KD vs. vps16 KD dlg KD</td><td>0.3902</td></tr></table></td></tr>
<tr><td></td><td>J</td><td>Central DCP-1 enrichment (Ptc stripe / WT); Individual units: Wing discs; n=8 for shi KD, n=6 for shi KD grnd KD; Values: Ratio of mean fluorescence measurements of cells in the wing pouch on 16-bit images; Two-sided Student’s T-test; t=4.035; DF=12

<table><tr><td>Comparison</td><td>P value</td></tr><tr><td>shi KD vs. shi KD grnd KD</td><td>0.0017</td></tr></table></td></tr>
<tr><td>S5</td><td>E</td><td>Grnd fluorescence (clones / WT); Individual units: Wing discs; n=19 for hsflpout ctrl, n=12 for hsflpout dlg KD; Values: Ratio of mean fluorescence measurements of cells in the wing pouch on 16-bit images; Two-sided Student’s T-test; t=6.857; DF=29

<table><tr><td>Comparison</td><td>P value</td></tr><tr><td>hsflpout ctrl vs. hsflpout dlg KD</td><td><0.0001</td></tr></table></td></tr>
</table>

F

Grnd fluorescence (Ptc stripe / WT); Individual units: Wing discs; n=13 for ptc> ctrl, n=22 for ptc> dlg KD, n=17 for ptc> dlg KD tak1 KD; Values: Ratio of mean fluorescence measurements of cells in the wing pouch on 16-bit images; Ordinary one-way ANOVA test, Tukey's multiple comparisons; P<0.0001; F=127.60; DF=51

Multiple comparisons	P value
ptc> ctrl vs. ptc> dlg KD	<0.0001
ptc> ctrl vs. ptc> dlg KD tak1 KD	0.7813
ptc> dlg KD vs. ptc> dlg KD tak1 KD	<0.0001

H

Grnd fluorescence (posterior / anterior); Individual units: Wing discs; n=5 for ctrl, n=6 for tak1 KD; Values: Ratio of mean fluorescence measurements of cells in the wing pouch on 16-bit images; Two-sided Student's T-test; t=5.707; DF=9

Comparison	P value
ctrl vs. tak1 KD	0.0003

K

RFP+ area / pouch area; Individual units: Wing discs; n=20 for ctrl, n=12 for grnd O/E; Values: Ratio of area measurements of cells in the wing pouch; Two-sided Student's T-test; t=0.2734; DF=30

Comparison	P value
ctrl vs. grnd O/E	0.7864

<table>
<tr><td></td><td>M</td><td>Grnd fluorescence (clones / WT); Individual units: Wing discs; n=9 for ctrl, n=12 for grnd O/E, n=12 for dlg KD; Values: Ratio of mean fluorescence measurements of cells in the wing pouch on 16-bit images; Ordinary one-way ANOVA test, Tukey’s multiple comparisons; P<0.0001; F=110.5; DF=32

<table><tr><td>Multiple comparisons</td><td>P value</td></tr><tr><td>ctrl vs. grnd O/E</td><td><0.0001</td></tr><tr><td>grnd O/E vs. dlg KD</td><td><0.0001</td></tr></table></td></tr>
<tr><td></td><td>N</td><td>EgrV fluorescence (clones / WT); Individual units: Wing discs; n=11 for ctrl, n=11 for grnd O/E, n=12 for dlg KD; Values: Ratio of mean fluorescence measurements of cells in the wing pouch on 16-bit images; Ordinary one-way ANOVA test, Tukey’s multiple comparisons; P=0.0002; F=10.95; DF=39

<table><tr><td>Multiple comparisons</td><td>P value</td></tr><tr><td>ctrl vs. dlgKD</td><td>0.0002</td></tr><tr><td>grnd O/E vs. dlg KD</td><td>0.0343</td></tr></table></td></tr>
<tr><td>S6</td><td>F</td><td>EgrGFP fluorescence (Ptc stripe / WT); Individual units: Wing discs; n=8 for ctrl, n=8 for dlg KD; Values: Ratio of mean fluorescence measurements of cells in the wing pouch on 16-bit images; Two-sided Student’s T-test; t=0.6405; DF=14

<table><tr><td>Comparison</td><td>P value</td></tr><tr><td>ctrl vs. dlg KD</td><td>0.5322</td></tr></table></td></tr>
</table>

G

EgrLacZ fluorescence (Ptc stripe / WT); Individual units: Wing discs; n=5 for ctrl, n=4 for dlg KD, n=5 for wounded; Values: Ratio of mean fluorescence measurements of cells in the wing pouch on 16-bit images; Ordinary one-way ANOVA test, Tukey's multiple comparisons; P=0.5471; F=0.6374; DF=13

Multiple comparisons	P value
ctrl vs. dlg KD	0.7992
ctrl vs. wounded	0.8662
dlg KD vs. wounded	0.5171

K

EgrLacZ fluorescence (mean of fat body cells per animal) ; Individual units: Fat body cells; n=9 for ctrl, n=5 for dlg KD, n=4 for wounded; Values: Mean fluorescence per fat body cell was measured on 16-bit images and the mean value per animal calculated (representing one data point); Ordinary one-way ANOVA test, Dunnett's multiple comparisons; P=0.7695; F=0.2666; DF=17

Multiple comparisons	P value
ctrl vs. dlg KD	0.7759
ctrl vs. wounded	>0.9999

<table>
<tr>
<td></td>
<td>P</td>
<td>EgrLacZ fluorescence (mean of hemocytes per bleed); Individual units: Hemocyte cells; n=3 for ctrl, n=3for dlg KD; Values: Mean fluorescence per hemocytes was measured on 16-bit images and the mean value per bleed calculated (representing one data point); Two-sided Student’s T-test; t=1.538; DF=4
<table>
<tr><td>Comparison</td><td>P value</td></tr>
<tr><td>ctrl vs. dlg KD</td><td>0.1988</td></tr>
</table>
</td>
</tr>
<tr>
<td></td>
<td>Q</td>
<td>EgrGFP fluorescence (mean of hemocytes per bleed); Individual units: Mean value of hemocytes per bleed; n=15 for ctrl, n=16 for dlg KD; Values: Mean fluorescence per hemocytes was measured on 16-bit images and the mean value per bleed calculated (representing one data point); Two-sided Student’s T-test; t=0.9578; DF=29
<table>
<tr><td>Comparison</td><td>P value</td></tr>
<tr><td>ctrl vs. dlg KD</td><td>0.3461</td></tr>
</table>
</td>
</tr>
<tr>
<td>S7</td>
<td>J</td>
<td>Grnd fluorescence (Ptc stripe / WT); Individual units: Wing discs; n=13 for ctrl, n=8 for cor KD; Values: Ratio of mean fluorescence measurements of cells in the wing pouch on 16-bit images; Two-sided Student’s T-test; t=6.341; DF=19
<table>
<tr><td>Comparison</td><td>P value</td></tr>
<tr><td>ctrl vs. cor KD</td><td><0.0001</td></tr>
</table>
</td>
</tr>
</table>

<table>
<tr>
<td>S9</td>
<td>B</td>
<td>EgrV fluorescence (mean); Individual units: Wing discs; n=6 for ctrl, n=8 for scrib -/- ; Values: Mean fluorescence measurements of the entire wing disc on 16-bit images; Two-sided Student’s T-test; t=7.472; DF=12

<table>
<tr><td>Comparison</td><td>P value</td></tr>
<tr><td>ctrl vs. scrib -/-</td><td><0.0001</td></tr>
</table>
</td>
</tr>
<tr>
<td></td>
<td>E</td>
<td>PH3+ cells per area; Individual units: Peripheral and core tissue regions of wing disc tumors; n=18 for scrib-/- periphery, n=18 for scrib-/- core, n=18 for FB>egr KD scrib-/- periphery, n=18 for FB>egr KD scrib-/- core; Values: Counted PH3+ cells per area in the tumor periphery or core; Ordinary one-way ANOVA test, Tukey’s multiple comparisons; P<0.0001; F=8.309; DF=71

<table>
<tr><td>Multiple comparisons</td><td>P value</td></tr>
<tr><td>scrib-/- periphery vs. FB>egr KD scrib-/- periphery</td><td><0.0001</td></tr>
<tr><td>FB>egr KD scrib-/- periphery vs.

FB>egr KD scrib-/- core</td><td>0.0480</td></tr>
<tr><td>scrib -/- core vs. FB>egr KD scrib-/- core</td><td>0.6269</td></tr>
</table>
</td>
</tr>
</table>